Bone 122 (2019) 199–208

Contents lists available at ScienceDirect

Bone

journal homepage: www.elsevier.com/locate/bone

Full Length Article

Discovery and validation an eight-biomarker serum gene signature for the diagnosis of steroid-induced osteonecrosis of the femoral head

Taixian Li[a,b,1], Yanqiong Zhang[a,1], Rongtian Wang[b], Zhipeng Xue[b], Shangzhu Li[c], Yuju Cao[d], Daobing Liu[b], Yanfang Niu[b], Xia Mao[a], Xiaoyue Wang[a], Weijie Li[a], Qiuyan Guo[a], Minqun Guo[a], Na Lin[a,*], Weiheng Chen[b,*]

[a] Institute of Chinese Materia Medica, China Academy of Chinese Medical Sciences, Beijing 100700, China
[b] Wangjing Hospital, China Academy of Chinese Medical Sciences, Beijing 100102, China
[c] Institute of Hematology & Blood Diseases Hospital, Chinese Academy of Medical Sciences, Peking Union Medical College, Tianjin 300041, China
[d] Zhengzhou Traditional Chinese Medicine Traumatology Hospital, Zhengzhou 450000, China

ARTICLE INFO

Keywords:
Steroid-induced osteonecrosis of the femoral head
Gene expression profiling
Biological molecular network
Biomarker
Partial least square model

ABSTRACT

Steroid-induced osteonecrosis of the femoral head (SONFH) is difficult to be diagnosed at the early stages when it can be administrated effectively. Yet, to date no study has been performed to identify diagnostic biomarkers and to develop diagnostic models for SONFH. In the current study, a total of 60 SONFH patients with Association Research Circulation Osseous (ARCO) stages I–IV, and 20 controls were enrolled and divided into the discovery and validation cohorts. The serum samples were collected and the gene expression profiles were detected by microarray analysis based on the discovery cohort. Then, eight genes (BIRC3, CBL, CCR5, LYN, PAK1, PTEN, RAF1 and TLR4) were identified as the candidate serum biomarkers of SONFH due to the significant differential expression patterns and the topological importance in the interaction network of SONFH-related differentially expressed genes. Functionally, these candidate serum biomarkers were significantly involved into several pathological processes during SONFH progression, such as the immune regulation and inflammation, bone metabolism and angiogenesis. After that, a prediction model for the diagnosis of SONFH was constructed using Partial least squares regression based on the serum levels of the candidate biomarkers. Notably, both the 10-fold cross-validation and the independent dataset test demonstrated the good performance of this model. In conclusion, our study discovered eight promising serum biomarkers and developed the multi-biomarker-based prediction model as a new, potential and non-invasive diagnostic tool for the detection of SONFH, as well as benefit the administration of SONFH in a daily clinical setting.

1. Introduction

Osteonecrosis of the femoral head (ONFH) represents femoral head partial blood circulatory disorder leading to the ischemia and necrosis of bone [1]. Statistically, > 80% of ONFH patients may progress to collapse and secondary hip arthritis without any intervention [2,3], which eventually result in progressive functional limitations and even disability [4]. Recent epidemiological surveys have indicated that ONFH may afflict > 20 million of people worldwide, 5–7.5 million in China [5]. Steroid-induced osteonecrosis of the femoral head (SONFH) is one of non-traumatic osteonecrosis of the femoral head with the top incidences of ONFH, and makes up 24.40%–51% of totally ONFH cases [6,7]. In clinics, SONFH is usually asymptomatic at the early stage and is difficult to be diagnosed, therefore, the femoral head of some patients have already collapsed at the diagnostic stage [8]. Once the collapse of the femoral head appears, the course of the disease is hard to be reversed [9]. Although the improvements in prosthetic and surgical techniques have improved the life quality of SONFH patients, a number of SONFH patients may face the psychological and economic burdens of revision arthroplasty after total hip arthroplasty [10], which is considered as definitive therapy of the ONFH patients. In addition, growing clinical evidence shows that joint-preserving procedures can lead to successful outcomes when they are used to pre-collapse stage of ONFH [11]. Therefore, it is of great clinical significance to identify novel

* Corresponding authors at: Institute of Chinese Materia Medica, China Academy of Chinese Medical Sciences, No. 16, Nanxiaojie, Dongzhimennei, Beijing 100700, China; Wangjing Hospital, China Academy of Chinese Medical Sciences, Huajiadijie, Chaoyangqu, Beijing 100102, China.
E-mail addresses: nlin@icmm.ac.cn (N. Lin), drchenweiheng@163.com (W. Chen).
[1] First author.

https://doi.org/10.1016/j.bone.2019.03.008
Received 5 January 2019; Received in revised form 4 March 2019; Accepted 6 March 2019
Available online 08 March 2019

biomarkers for the diagnosis of SONFH in order to prevent collapse and delay disease progression effectively.

Accumulating studies have revealed that the development and progression of SONFH may be associated with the maximum daily dose, the total cumulative dose and the duration of steroid treatment [12–15]. Several genetic factors, such as matrix metallopeptidase 9, SMAD family member 3, peroxisome proliferator-activated receptor gamma and gremlin 1, etc., were indicated as key players during SONFH progression [16–18]. Our previous studies also found that single nucleotide polymorphism (SNP) (rs1045642) of the P-glycoprotein gene ABCB1 [19], SNP (rs662) of the PON-1 gene [20], SNP (rs2227631) of plasminogen activator inhibitor-1 [21] were associated with the risk of SONFH. However, little comprehensive investigation by high-throughput platforms have been performed on SONFH, and potential interactions among differentially expressed genes (DEGs) of different disease stages were not taken into consideration.

Since microarray technology combined with molecular interaction network analysis allows systematic investigation of disease-related genes, in the current study, a total of 60 SONFH patients with Association Research Circulation Osseous (ARCO) stages I–IV, and 20 controls were enrolled and divided into the discovery cohort and the validation cohort (Step 1, Fig. 1). The serum samples were collected and the gene expression profiles were detected by microarray analysis based on the discovery cohort (Step 2, Fig. 1). Then, a list of candidate serum biomarkers of SONFH were identified by integrating differential expression data analysis and gene signal transduction network analysis (Step 3, Fig. 1). After that, a prediction model for the diagnosis of SONFH was constructed using PLS regression based on the serum levels of the candidate biomarkers, and also evaluated by both 10-fold cross-validation and independent dataset test (Step 4, Fig. 1).

2. Methods

2.1. Ethics statement

The study was approved by the Research Ethics Committee of Institute of Chinese Materia Medica, Wangjing Hospital, China (SFDA approval number: 81473695). The informed consent was obtained from all patients.

2.2. Study subjects

A total of 60 SONFH patients with various indications for steroid treatment, including autoimmune diseases [systemic lupus erythematosus (n = 20)], renal diseases [nephritic syndrome (n = 11), pyelonephritis (n = 3), IgA nephropathy (n = 3), chronic nephritis (n = 2) and interstitial nephritis (n = 1)], dermatogic diseases [allergic dermatitis (n = 3), psoriasis (n = 4), tinea manus and pedis (n = 1), seborrheic dermatitis (n = 2), skin pruritus (n = 1), eczema (n = 4), urticaria (n = 3), lichen simplex chronicus (n = 1) and neurodermatitis (n = 1)], were collected from August 2015 to October 2017 in Wangjing Hospital and Zhengzhou Traditional Chinese Medicine Traumatology Hospital. For the control group, 20 patients who received steroid administration against hematologic diseases [thrombocytopenic purpura (n = 4), pure red cell aplasia (n = 3), acute lymphocytic leukemia (n = 13)], but not developed SONFH, were collected from August 2015 to October 2017 in Institute of Hematology & Blood Diseases Hospital of China Academy of Chinese Medical Sciences. Inclusion Criteria of our cohorts included (1) ONFH patients was diagnosed based on the Mont MA presented criteria [22]; (2) Staging criteria of ONFH were based on ARCO [23]; (3) No demonstrable history of direct trauma; (4) A demonstrable history of application of steroid therapy; (5) All SONFH patients were diagnosed for the first visit. All 80 patients were randomly divided into the discovery cohort (n = 40, including ARCO stages I–II, stage III, stage IV and control groups, 10 per group) and the validation cohort (n = 40, including ARCO stages I–II, stage III, stage IV and control groups, 10 per group). Among them, 40 individual samples of the discovery cohort were used to perform microarray analysis and construct the SONFH prediction model; 40 individual samples of the validation cohort were used to verify the expression patterns of the candidate gene biomarkers of SONFH by qPCR analysis, and also evaluate the performance of our SONFH prediction model by independent dataset validation. There are no significant differences in clinical parameters between the discovery cohort and the validation cohort. The clinical characteristics of our cohorts were summarized in Table 1.

2.3. Gene expression profiling

The serum samples (2.5 mL) were collected from both discovery and validation cohorts and stored in PAXgene Blood RNA Tube (Cat#762165, PreAnalytiX, GmbH, UK). Total RNA was extracted and

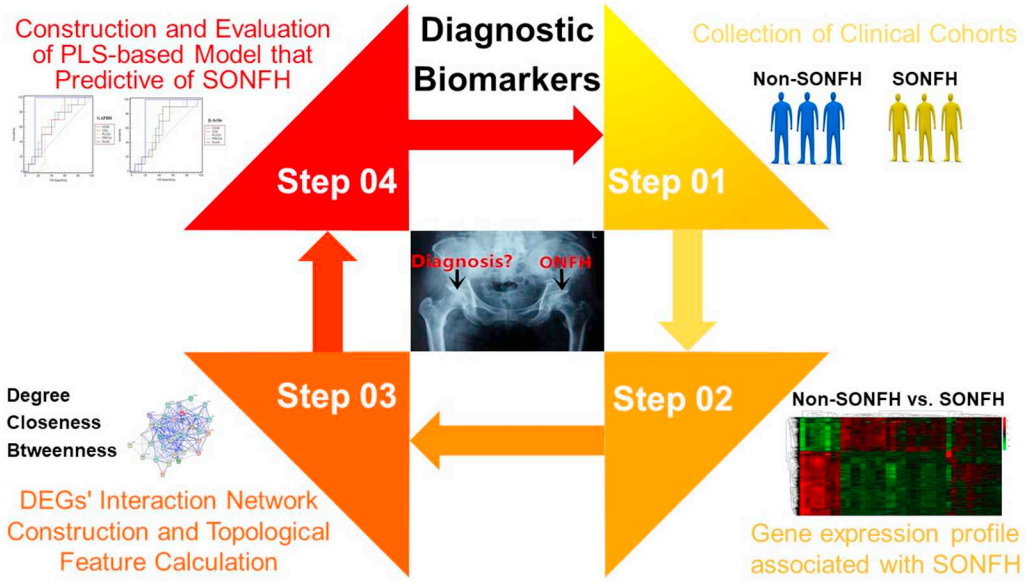

Fig. 1. A schematic diagram of the systematic strategies to identify potential gene biomarkers and to construct PLS-based model that predictive of SONFH.

Table 1
Clinical information of study subjects.

Baseline variables	Discovery cohort			Validation cohort		
	SONFH group	Non-SONFH group	P	SONFH group	Non-SONFH group	P
Gender						
Male	13	7	0.14	11	5	0.46
Female	17	3		19	5	
Body mass index, (BMIkg/m^2)						
Median (range)	24.09(18.82–34.72)	24.21(21.09–28.91)	/	22.99(18.42–28.23)	25.02(20.83–29.27)	/
Mean	23.07 ± 3.01	25.02 ± 2.87	0.90	24.09 ± 3.65	23.91 ± 1.39	0.97
Age (year)						
Median (range)	39.6(21–74)	34.0(17–57)	/	41.17(20–66)	38.8(23–57)	/
Mean	41.17 ± 12.57	38.80 ± 10.86	0.53	39.60 ± 13.56	34.00 ± 15.54	0.50
ARCO stage						
ARCO I–II	10	0	/	10	0	/
ARCO III	10	0		10	0	
ARCO IV	10	0		10	0	
Steroid treatment						
Drug species	Prednisone; methylprednisolone; dexamethasone; halometason	Prednisone; methylprednisolone; dexamethasone	/	Prednisone; methylprednisolone; dexamethasone	Prednisone; methylprednisolone; dexamethason	/
Duration of steroid treatment (month)						
Median (range)	34.1(2−112)	17.2(12−120)	/	25.4(1–108)	28.3(5–60)	/
Mean	25.27 ± 22.24	28.30 ± 36.07	0.21	34.90 ± 30.53	17.20 ± 3.74	0.55

purified using PAXgene Blood RNA Kit (Cat#762174, QIAGEN, GmBH, Germany) following the manufacturer's instructions. RIN number was detected to evaluate RNA integration by an Agilent Bioanalyzer 2100 (Agilent technologies, Santa Clara, CA, US). The concentration of total RNA was measured using a NanoDrop spectrophotometer (Nanodrop technologies, Montchanin, DE, USA). Total RNA was eluted in 15 μl of RNase-free water and stored at −80 °C.

Gene expression profiles were detected by PrimeView Human Gene Expression carried out by Shanghai Biotechnology Corporation, Shanghai, China. The gene expression microarray data of GSE123568 are provided in National Center of Biotechnology Information Gene Expression Omnibus (https://www.ncbi.nlm.nih.gov/geo/query/acc.cgi?acc=GSE123568).

DEG Screening.

The signal intensities on microarray for 40 samples were normalized by Robust Multi-array Average (RMA), and 10 Non-SONFH samples were used for baseline signal intensity. DEGs between SONFH and non-SONFH groups were identified using the criteria of |log2 fold change (FC)| > 1.15, P value < 0.05 by the RVM *t*-test. The heat map, an R package was used for the hierarchical clustering analysis.

2.4. Gene signal transduction network analysis

Gene signal transduction network associated with SONFH development and progression was constructed using the interactions among DEGs between SONFH and non-SONFH groups, according to the interaction data obtained from the public database STRING (Search Tool for Known and Predicted Protein-Protein Interactions, version 10.0, http://string-db.org/) [24]. Highly reliable gene-gene interaction data with a combined evidence score higher than the median value of all scores were selected. In the network, nodes referred to DEGs between SONFH and non-SONFH groups, and edges referred to interactions between the nodes. In order to identify the candidate gene biomarkers of SONFH, three topological features, including degree, betweenness and closeness, were calculated according to our previous studies [25,26].

2.5. Functional enrichment analysis

To investigate the pathways involved by the candidate gene biomarkers of SONFH, a pathway enrichment analysis was performed using the Database Visualization and Integrated Discovery software (DAVID, http://david.abcc.ncifc rf.gov/home.jsp, version 6.7) based on the biological process data collected from Gene Ontology Consortium (GO, http://www.geneontology.org/, updated on November 2, 2016) and the pathway data obtained from the Kyoto Encyclopedia of Genes and Genomes database (KEGG, http://www.genome.jp/kegg/, updated on November 18, 2016) [27,28]. The pathway annotations were chosen for further analysis only if the enrichment P values were < 0.05 following the correction by both algorithms of Bonferroni and Benjamini (P < 0.05).

2.6. Quantitative PCR analysis

To verify the expression patterns of the candidate gene biomarkers of SONFH, quantitative PCR analysis was performed using the serum samples obtained from the validation cohort. Both GAPDH and β-actin were used as two internal controls for candidate gene expression normalization and quantification. Quantitative PCR analysis and data collection were performed on the ABI 7900HT qPCR system using the primer pairs listed in Additional File 1. Relative quantification of gene expression was evaluated using the comparative cycle threshold (CT) method. The raw quantifications were respectively normalized to GAPDH and β-actin values for each sample and fold changes were shown as mean ± SD in three independent experiments with each triplicate.

2.7. Construction and Performance Evaluation of the Eight-Biomarker Serum Gene Signature-based prediction model for the diagnosis of SONFH

Following the identification of candidate serum biomarkers, a SONFH prediction model was constructed using the PLS algorithm based on the serum levels of candidate biomarkers according to our previous studies [29].

Ten-fold cross-validation [30] and independent dataset test [31] were both performed to evaluate the performance of our SONFH prediction model according to the previous studies [25,26]. In brief, for 10-fold cross-validation, the samples of the discovery cohort were randomly divided into two parts: training dataset and testing dataset. The training dataset was used to calculate the weight values of the

candidate gene biomarkers of SONFH and the cutoff point of the model. The test dataset was used to evaluate the performance of the model. This process was repeated for 10 times. For the independent dataset test, the serum levels of the candidate gene biomarkers were detected using the validation cohort and were used to evaluate the performance of our model.

For evaluating the performance of our SONFH prediction model, the average accuracy, sensitivity and specificity, as well as the average area-under-curve (AUC) from receiver-operating-characteristic (ROC) curves were calculated as the following formulas:

$$Sensitivity = \frac{TP}{TO + FN} \quad (1)$$

$$Specificity = \frac{TN}{TN + FN} \quad (2)$$

$$Accuracy = \frac{\sum TP + TN}{N} \quad (3)$$

where TP, TN, FP, FN respectively refer to the number of true positive, true negative, false positive and false negative result components in a test, while *N* refers to the total number of predicted samples.

2.8. Statistical analysis

Statistical analysis was performed using SPSS software (Version 13.0, Statistical Program for Social Sciences, Inc.: Chicago, IL, USA). Continuous variables were expressed as $\bar{x} \pm s$. Measurement data and enumeration data were respectively statistically analyzed using *t*-tests and χ^2 test. Expression levels of candidate gene biomarkers between SONFH and non-SONFH groups were compared by one-way analysis of variance. P-values < 0.05 were considered to be significant.

3. Results

3.1. DEGs in SONFH patients

A total of 1112 (including 604 upregulated and 508 downregulated) genes displayed the significantly differential expression patterns between SONFH and non-SONFH groups (all fold change > 1.15 and $P < 0.05$). The detailed information of DEGs is provided in Additional file 2.

The heat-map and the unsupervised hierarchical clustering of the above DEG profiles revealed distinctive patterns of SONFH and non-SONFH groups (Fig. 2A). Functionally, the DEGs of SONFH were significantly involved into bone metabolism-related pathways (such as thyroid hormone signaling pathway, regulation of myeloid cell differentiation, osteoclast differentiation, chondroitin sulfate metabolic process, chondroitin sulfate biosynthetic process, estrogen signaling pathway, podosome assembly, metabolism of xenobiotics by cytochrome P450, inositol phosphate metabolism, amyloid precursor protein catabolic process, amyloid precursor protein biosynthetic process, amyloid precursor protein metabolic process, FoxO signaling pathway, apoptosis), hematopoiesis and coagulation function-related pathways (such as regulation of lipid catabolic process, platelet activation, lipoprotein transport, hematopoietic cell lineage, notch signaling pathway, HIF-1 signaling pathway) and inflammatory response (such as TNF signaling pathway, NF-kappa B signaling pathway, leukocyte transendothelial migration), which are all significantly associated with SONFH development and progression (all $P < 0.05$, Fig. 2B and C).

3.2. Candidate serum biomarkers for diagnosis of SONFH

The interaction network of SONFH-related DEGs was constructed using the links among DEGs between SONFH and non-SONFH groups. A total of 202 hub genes, whose degree values were higher than two-fold the median of all degree values in the network, were identified. Then, the hub interaction network was constructed based on the direct interactions among the hub genes. There were 202 nodes and 2271 edges in the hub interaction network. Following the evaluation of their topological centrality by calculating the hubs' degree, betweenness and closeness (Additional file 3), 85 major hubs were selected and functionally divided into three network modules, which were respectively associated with immune regulation and inflammation, bone metabolism and angiogenesis (Fig. 3). The top eight hub genes with relatively high degree in the network were as follows: BIRC3 (degree = 20); CBL (degree = 33); CCR5 (degree = 35), LYN (degree = 47), PAK1 (degree = 31), PTEN (degree = 26), RAF1 (degree = 36) and TLR4 (degree = 29). Moreover, the results obtained from quantitative PCR analysis based on the validation cohort verified that the differential serum levels of BIRC3, CBL, CCR5, LYN, PAK1, PTEN, RAF1 and TLR4 normalized by GAPDH and β-actin were both consistent with that of microarray analysis (Fig. 4 and Table 2). Considering the differential expression patterns in SONFH sera, highly topological importance in disease-related network, as well as functional relevance to SONFH development and progression (Table 3), we selected BIRC3, CBL, CCR5, LYN, PAK1, PTEN, RAF1 and TLR4 as the candidate serum biomarkers for the SONFH diagnosis.

3.3. The Eight-Biomarker Serum Gene Signature-based PLS model shows the high efficiency to screen SONFH

To determine the application of the candidate serum biomarkers into the SONFH diagnosis, a PLS prediction model using the serum levels of BIRC3, CBL, CCR5, LYN, PAK1, PTEN, RAF1 and TLR4 was established. The values of weight for each candidate serum biomarkers and cutoff point of the model were trained by the discovery cohort. For β-actin as the internal control, the values of weight for BIRC3, CBL, CCR5, LYN, PAK1, PTEN, RAF1 and TLR4 were respectively −0.012, −0.329, −0.254, 0.332, 0.561, 0.422, 0.469 and −0.052. For GAPDH as the internal control, the values of weight for eight gene biomarkers were respectively −0.097, 0.019, −0.316, 0.292, 0.681, 0.375, 0.428 and 0.129. The cutoff points of the PLS model were 0.023 and 0.040, respectively, for β-actin and GAPDH as the internal controls, which means that the score of SONFH patients should be higher than the cutoff values.

To evaluate the prediction performance of our PLS model, the 10-fold cross-validation based on the discovery cohort and the independent dataset test based on the validation cohort were both performed. In the 10-fold cross-validation, the mean accuracy value of the PLS model was 91.20%, and the mean AUC values were 0.901. In the independent dataset test, the serum levels of eight candidate biomarkers (BIRC3, CBL, CCR5, LYN, PAK1, PTEN, RAF1, TLR4) detected by quantitative PCR analysis based on the validation cohort were used. The accuracy and AUC values of the PLS-based model based on the expression levels of the eight gene biomarkers using GAPDH as an internal control were respectively 95.00% and 0.857, which was consistent with the PLS-based model based on the serum levels of the eight gene biomarkers using β-actin as an internal control (the accuracy was 90.00% and the AUC value was 0.893).

Furthermore, we performed the ROC comparison to determine the necessity and effectiveness of the PLS-based model for the SONFH diagnosis. After comparing the performance of the eight candidate serum biomarkers alone to the PLS-based model which was integrated them, we found that the AUC values of the PLS-based model based on both GAPDH and β-actin were significantly higher than those of the single gene biomarker as shown in Fig. 5.

4. Discussion

Accumulating studies have performed gene expression microarray analyses on a genome-wide scale to screen crucial genes and pathways involved into the development, progression and prognosis of various

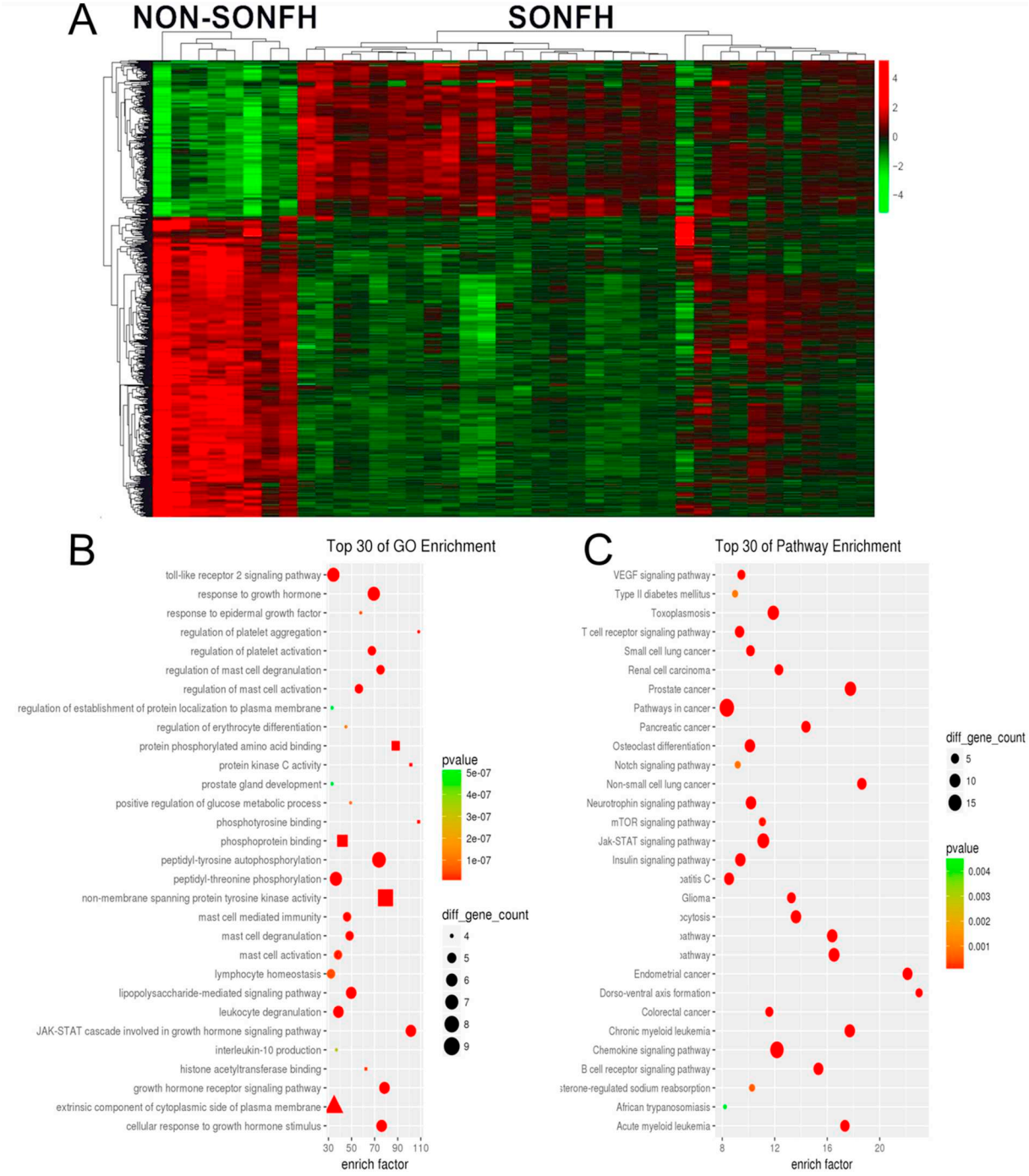

Fig. 2. DEGs associated with SONFH. (A) Heat map showing hierarchical clustering of mRNAs, whose expression changes were > 1.5-fold in the comparison between the disease and control groups. In clustering analysis, up- and down-regulated genes are colored in red and green, respectively. (B) and (C) Top 30 of GO items and KEGG pathways enriched by the DEGs in the comparison between the disease and control groups. (For interpretation of the references to color in this figure legend, the reader is referred to the web version of this article.)

diseases, including SONFH. However, different genes and pathways are often identified from individual studies due to the complicated pathogenesis and different detection platforms. To address this problem, we here proposed to conduct a systematical approach by integrating microarray detection, differential expression data screening, molecular interaction network analysis and bioinformatics prediction modeling for the identification of SONFH diagnostic biomarkers. The main findings of the present study are as follows: At first, the eight candidate serum biomarkers that were predictive of the occurrence of SONFH were identified according to their significantly differential expression patterns in patients' sera based on both the discovery cohort and the validation cohort, as well as highly topological importance in the disease-related network. Then, the PLS algorithm was applied to establish the SONFH diagnostic model based on the serum levels of the eight candidate gene biomarkers. Notably, both 10-fold cross-validation and the independent dataset test verified the favorable performance of this model in discriminating the patients with SONFH from controls in the general population. Moreover, we also verified a distinguished improvement of the PLS-model based on the serum levels of the eight candidate biomarkers in combination over the gene biomarkers alone,

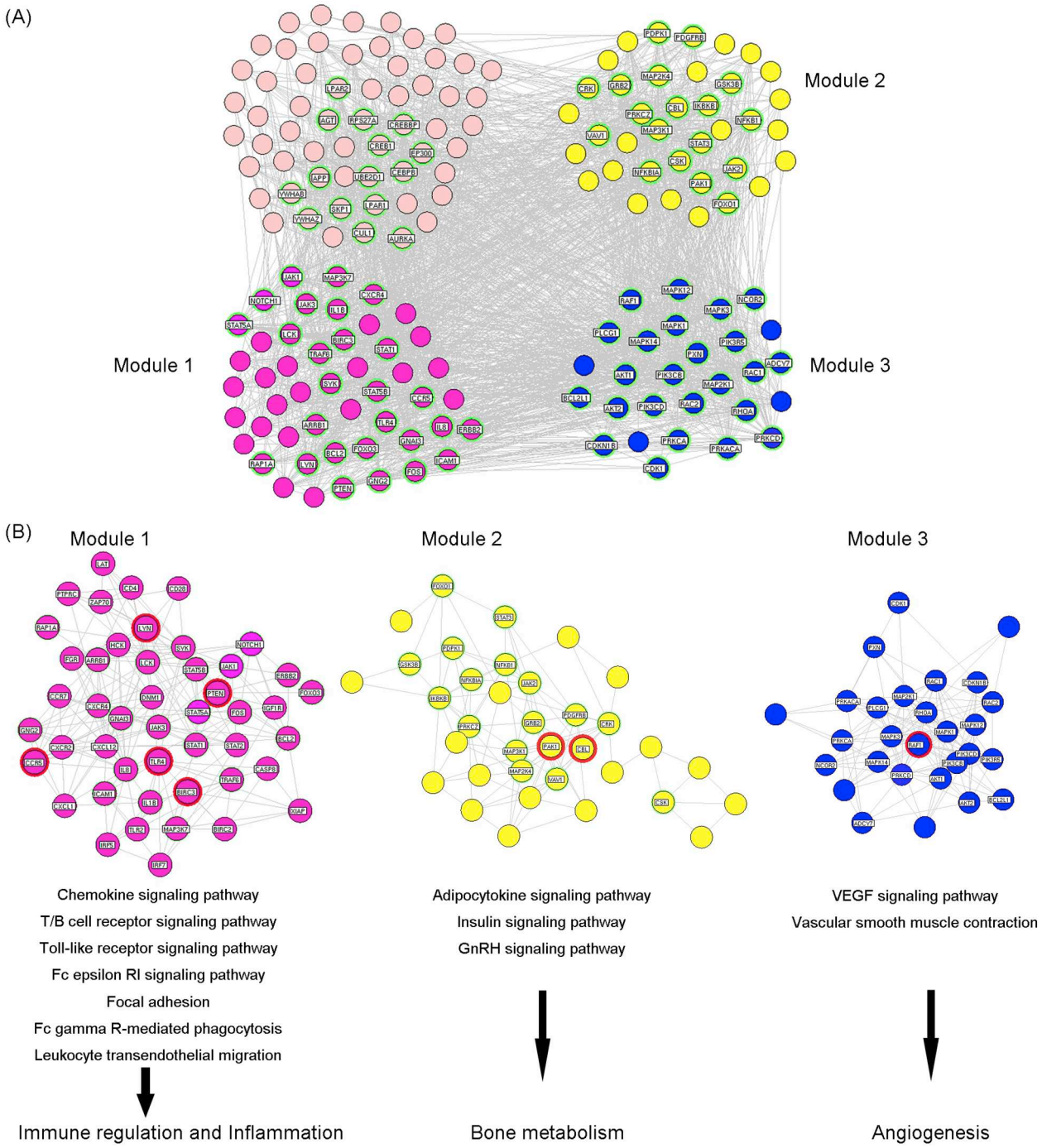

Fig. 3. The interaction network of SONFH-related DEGs and three functional modules associated with SONFH-related pathways. (A) The interaction network of SONFH-related DEGs constructed using the links among DEGs between SONFH and non-SONFH groups. (B) Three functional network modules, which were respectively associated with immune regulation and inflammation, bone metabolism and angiogenesis.

in predicting SONFH, suggesting the rationality of our modeling design.

Microarray technology combined with bioinformatics and molecular interaction network analyses may illustrate the comprehensive map of gene expression changes and functional properties. Therefore, it is a useful strategy to systematically understand disease occurrence and progression. In the current study, we successfully introduced this systems biology-based approach to explore the candidate gene biomarkers for the diagnosis of SONFH: BIRC3, CCR5, CBL, LYN, PAK1, TLR4, RAF1 and PTEN. Among them, BIRC3 (Baculoviral IAP Repeat Containing 3) encodes a member of the Inhibitors of apoptosis proteins (IAP) family of proteins that inhibit apoptosis by binding to tumor necrosis factor receptor-associated factors TRAF1 and TRAF2. It exerts ligase activity and cysteine-type endopeptidase inhibitor activity involved into Focal Adhesion and NF-kappa B signaling pathway [32,33]. CBL (Cbl Proto-Oncogene) is a proto-oncogene that encodes a RING finger E3 ubiquitin ligase, which is one of the enzymes required for targeting substrates for degradation by the proteasome. It plays a role in Immune response Fc epsilon RI pathway and EGF/EGFR Signaling Pathway via showing the DNA binding transcription factor activity and ligase activity [34]. Cao et al. [35] indicated that the decreased expression of CBL inhibits VEGF-induced vascular hyperpemeability and osteoclast activity, which may be in advantage of the renovation of

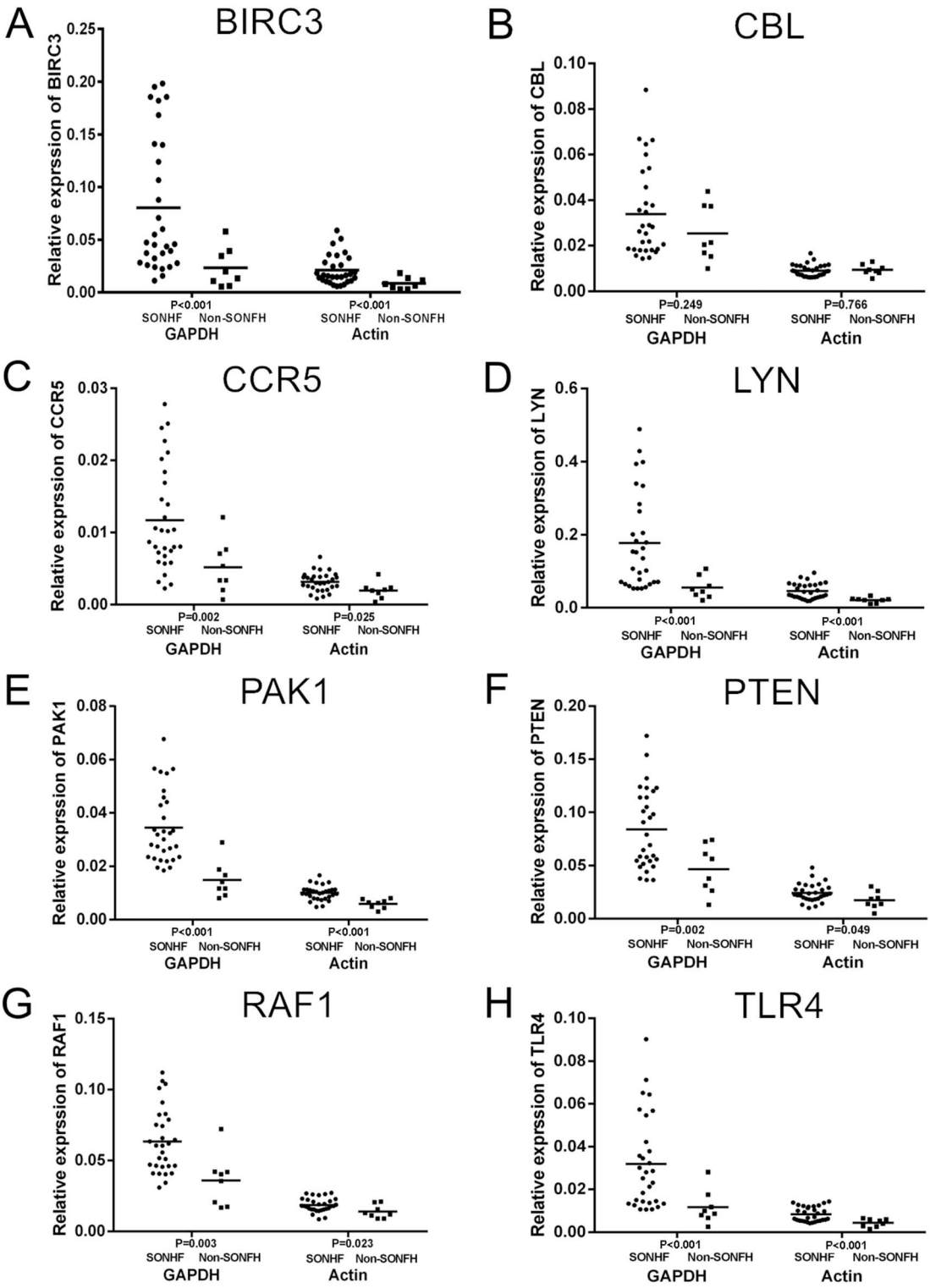

Fig. 4. Serum levels of the eight candidate gene biomarkers (A, BIRC3; B, CBL; C, CCR5; D, LYN; E, PAK1; F, PTEN; G, RAF1; H, TLR4) in SONFH and non-SONFH patients using GAPDH and β-actin as internal control in quantitative PCR analysis.

femoral head necrosis. In addition, its related pathways EGF/EGFR [36] and Immune response Fc epsilon RI [37] may play a crucial role in the immune system and bone formation, microvascularization. CCR5 (C—C Motif Chemokine Receptor 5) encodes a member of the beta chemokine receptor family and is expressed by T cells and macrophages [38]. Lee et al.[39] found that CCR5 was implicated into bone-destructive diseases via regulating osteoclasts. Moreover, the activation of Akt Signaling pathway, one of CCR5-related pathway, was revealed to promote angiogenesis and prevent bone loss in ONFH [40]. LYN (LYN Proto-Oncogene, Src Family Tyrosine Kinase) encodes a tyrosine protein kinase and RAF1(Raf-1 Proto-Oncogene, Serine/Threonine Kinase) encodes a MAP kinase kinase kinase (MAP3K). Both of LYN and RAF1 are involved in the regulation of Immune response Fc epsilon RI pathway. Okazaki et al. [41] reported that ONFH may be caused by the disruption of the immune system involved by LYN and RAF1. PAK1 (P21 Activated Kinase 1) encodes a family member of serine/threonine p21-activating

Table 2
The differential serum levels of the top eight hub genes from quantitative PCR analysis based on the validation cohort.

Gene	Internal control	Group	Serum levels	P
BIRC3	Gapdh	SONFH group	0.080 ± 0.063	< 0.001
		Non-SONFH group	0.023 ± 0.018	
	Actin	SONFH group	0.021 ± 0.013	< 0.001
		Non-SONFH group	0.008 ± 0.026	
CBL	Gapdh	SONFH group	0.034 ± 0.019	0.249
		Non-SONFH group	0.025 ± 0.012	
	Actin	SONFH group	0.009 ± 0.002	0.766
		Non-SONFH group	0.009 ± 0.002	
CCR5	Gapdh	SONFH group	0.011 ± 0.007	0.002
		Non-SONFH group	0.005 ± 0.003	
	Actin	SONFH group	0.003 ± 0.001	0.025
		Non-SONFH group	0.001 ± 0.001	
LYN	Gapdh	SONFH group	0.176 ± 0.130	< 0.001
		Non-SONFH group	0.054 ± 0.030	
	Actin	SONFH group	0.045 ± 0.021	< 0.001
		Non-SONFH group	0.020 ± 0.007	
PAK1	Gapdh	SONFH group	0.034 ± 0.013	< 0.001
		Non-SONFH group	0.014 ± 0.006	
	Actin	SONFH group	0.010 ± 0.002	< 0.001
		Non-SONFH group	0.005 ± 0.001	
PTEN	Gapdh	SONFH group	0.084 ± 0.037	0.002
		Non-SONFH group	0.046 ± 0.022	
	Actin	SONFH group	0.024 ± 0.008	0.049
		Non-SONFH group	0.017 ± 0.008	
RAF1	Gapdh	SONFH group	0.063 ± 0.022	0.003
		Non-SONFH group	0.035 ± 0.018	
	Actin	SONFH group	0.018 ± 0.004	0.023
		Non-SONFH group	0.013 ± 0.004	
TLR4	Gapdh	SONFH group	0.031 ± 0.021	< 0.001
		Non-SONFH group	0.016 ± 0.007	
	Actin	SONFH group	0.008 ± 0.003	< 0.001
		Non-SONFH group	0.004 ± 0.001	

Table 3
The involved pathways and the relevance to SONFH of the candidate gene biomarkers.

Gene biomarkers	Pathways	Relevance to SONFH
BIRC3	Focal adhesion	Osteocyte metabolism
	NF-kappa B	Inflammation
CBL	Immune response Fc epsilon RI	Reflect underlying diseases of steroid treatment
	EGF/EGFR	Osteoblast differentiation and bone resorption
CCR5	Akt signaling	Angiogenesis
		Inhibition osteoclast differentiation
LYN	Immune response Fc epsilon RI	Reflect underlying diseases of steroid treatment
	CD209 (DC-SIGN)	Inflammation
PAK1	Focal adhesion	Osteocyte metabolism
PTEN	ERK	Chondrocyte anabolism
RAF1	Focal adhesion	Osteocyte metabolism
	Immune response Fc epsilon RI	Reflect underlying diseases of steroid treatment
TLR4	MIF action through endocytic	Counteract the anti-inflammatory effect of corticosteroids

kinases, which are critical effectors that link RhoGTPases to cytoskeleton reorganization and nuclear signaling, and serve as targets for the small GTP binding proteins Cdc42 and Rac [42]. PAK1 exerts transferase activity and protein tyrosine kinase activity, as well as plays a role in Focal Adhesion Pathway. PTEN (Phosphatase And Tensin Homolog) was identified as a tumor suppressor that is mutated in a large number of cancers at high frequency. It is a part of the PI3K/AKT/mTOR pathway and mTOR inhibitors have been relatively ineffective in treating patients with PTEN loss [43]. Mollazadeh et al. [44] observed that PTEN expression could reduce the loss of bone mass through the deceleration of apoptosis, and its related ERK Signaling pathway have been revealed to have a positive effect on chondrocyte anabolism [45]. TLR4 (Toll Like Receptor 4) is a member of the Toll-like receptor (TLR) family which plays a fundamental role in pathogen recognition and activation of innate immunity. Accumulating studies have found the involvement of TLR4 into osteonecrosis. For example, Okazaki et al. [41] indicated that TLR4 might play an important role in corticosteroids induced osteonecrosis of the femoral head by disturbing the immune system. Adapala et al. [46] also found the relation between TLR4 and inflammatory responses to tissue necrosis. They revealed that TLR4 mediated macrophage-inflammatory responses to increased expression of IL-1β, TNF-α, and IL-6. The above literature reports support the evidence that the candidate gene biomarkers identified here may be associated with disease occurrence and progression of SONFH.

To determine the clinical utility of the candidate gene biomarkers, we built an auxiliary tool for SONFH diagnosis using the PLS algorithm, which can effectively differentiate two datasets by extracting effective information from a large number of features [47]. Notably, both 10 fold cross-validation and the independent dataset test demonstrated that our PLS model had the high predictive accuracy (81.34%–91.20%) and area under ROC curve (0.804–0.901) when it was used to screen SONFH patients from controls based on a large clinical cohort, suggesting it may offer a contribution to the diagnosis and prevention of femoral head collapse.

However, there was a limitation in the current study. Our SONFH cohorts contain various ARCO stages (I–IV), thus, the candidate gene biomarkers identified here might not represent the early stage of SONFH. Since all the SONFH patients were recruited when diagnosed at the first visit, our eight-biomarker serum gene signature may be used to improve the accurate diagnosis of SONFH patients when they are first visit to doctors.

5. Conclusions

The current study discovered eight promising serum biomarkers and developed the multi-biomarker-based prediction model as a new, potential and non-invasive diagnostic tool for the detection of SONFH, as well as benefits the administration of SONFH in a daily clinical setting. These biomarkers are useful but are not best early diagnosis of SONFH. Therefore, further research is needed to determine if the biomarkers and the prediction model could predict the early SONFH, and validation test are needed to perform on people who received steroid administration.

Acknowledgments

This study is funded by National Natural Science Foundation of China (No. 81373656 & 81473695) and Beijing Municipal Natural Science Foundation (No. 7182186).

Funding sources

The funding sources of this study are from National Natural Science Foundation of China and Beijing Municipal Natural Science Foundation. No study sponsors are involved in the research process of this project.

Declare of interests.

The authors declare that there is no conflict of interests regarding the publication of this paper.

Author contributions

Prof. Na Lin, Yanqiong Zhang and Weiheng Chen engaged in study design and coordination, material support for obtained funding, and supervised study. Prof. Na Lin and Weiheng Chen guided the experimental validation and revised the manuscript. Prof. Yanqiong Zhang performed network analysis, designed the experimental validation and

(A)

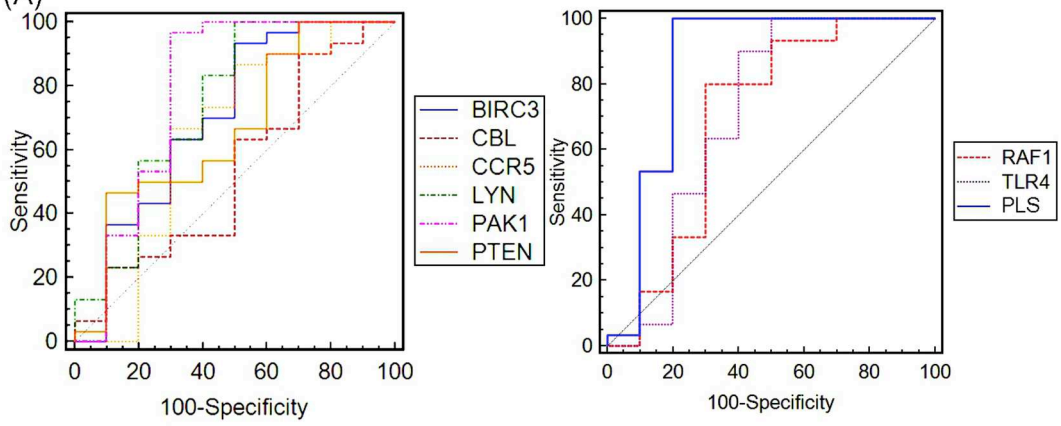

Genes/Model	AUC	SE	95% CI
BIRC3 *	0.703	0.0889	0.538 to 0.837
CBL **	0.537	0.105	0.372 to 0.695
CCR5 **	0.640	0.0968	0.473 to 0.785
LYN *	0.740	0.0833	0.577 to 0.865
PAK1 *	0.783	0.0757	0.625 to 0.897
PTEN **	0.663	0.0941	0.497 to 0.805
RAF1 *	0.697	0.0898	0.531 to 0.832
TLR4 *	0.707	0.0884	0.542 to 0.839
PLS	0.857	0.060	0.710 to 0.947

(B)

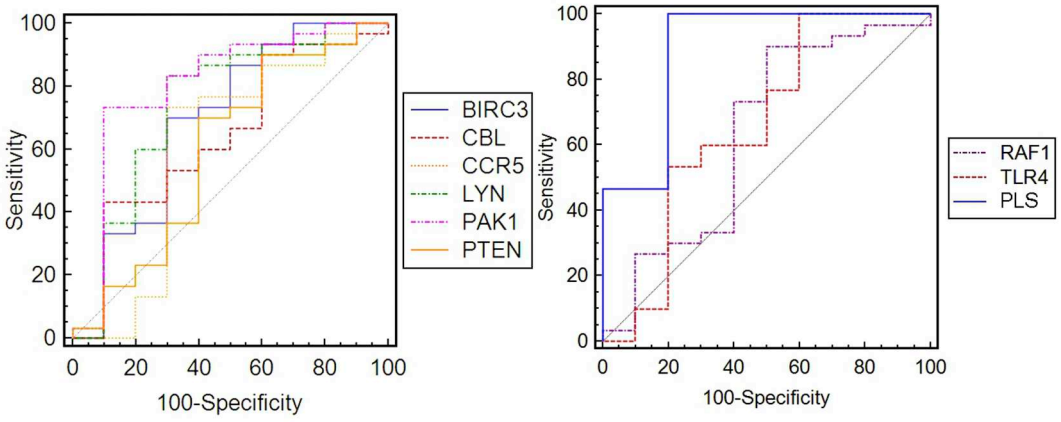

Genes/Model	AUC	SE	95% CI
BIRC3 **	0.693	0.0902	0.528 to 0.829
CBL **	0.640	0.106	0.473 to 0.785
CCR5 **	0.610	0.0997	0.443 to 0.760
LYN *	0.743	0.0827	0.581 to 0.868
PAK1 *	0.807	0.0711	0.651 to 0.914
PTEN **	0.597	0.101	0.430 to 0.748
RAF1 **	0.633	0.0975	0.466 to 0.780
TLR4 **	0.660	0.0945	0.493 to 0.802
PLS	0.893	0.0505	0.755 to 0.968

Fig. 5. ROC comparison on the performance of the eight candidate gene biomarkers alone to the PLS-based model which was integrated them based on GAPDH (A) and Actin (B) as internal controls. $^{*}P < 0.05$, $^{**}P < 0.01$, compared with the PLS-based model.

revised the manuscript. Dr. Taixian Li performed most of the experiments and statistical analysis, as well as wrote the manuscript. Dr. Rongtian Wang was responsible for collecting the clinical samples. The other authors performed parts of the experiments. All authors reviewed and approved the final manuscript.

Appendix A. Supplementary data

Supplementary data to this article can be found online at https://doi.org/10.1016/j.bone.2019.03.008.

References

[1] F. Liu, W. Wang, L. Yang, B. Wang, J. Wang, W. Chai, D. Zhao, An epidemiological study of etiology and clinical characteristics in patients with nontraumatic osteonecrosis of the femoral head, J. Res. Med. Sci. 22 (2017) 15.

[2] Y. Kuroda, S. Matsuda, H. Akiyama, Joint-preserving regenerative therapy for patients with early-stage osteonecrosis of the femoral head, Inflammation Regen. 36 (2016) 4.

[3] M.A. Mont, L.C. Jones, D.S. Hungerford, Nontraumatic osteonecrosis of the femoral head: ten years later, J. Bone Joint Surg. (Am. Vol.) 88 (2006) 1117–1132.

[4] C.G. Zalavras, J.R. Lieberman, Osteonecrosis of the femoral head: evaluation and treatment, J. Am. Acad. Orthop. Surg. (2015) 69–70.

[5] L. Cui, Q. Zhuang, J. Lin, J. Jin, K. Zhang, L. Cao, J. Lin, S. Yan, W. Guo, W. He, F. Pei, Y. Zhou, X. Weng, Multicentric epidemiologic study on six thousand three hundred and ninety five cases of femoral head osteonecrosis in China, Int. Orthop. 40 (2016) 267–276.

[6] D.W. Zhao, M. Yu, K. Hu, W. Wang, L. Yang, B.J. Wang, X.H. Gao, Y.M. Guo, Y.Q. Xu, Y.S. Wei, S.M. Tian, F. Yang, N. Wang, S.B. Huang, H. Xie, X.W. Wei, H.S. Jiang, Y.Q. Zang, J. Ai, Y.L. Chen, G.H. Lei, Y.J. Li, G. Tian, Z.S. Li, Y. Cao, L. Ma, Prevalence of nontraumatic osteonecrosis of the femoral head and its associated risk factors in the chinese population: results from a nationally representative survey, Chin. Med. J. 128 (2015) 2843–2850.

[7] T. Kubo, K. Ueshima, M. Saito, M. Ishida, Y. Arai, H. Fujiwara, Clinical and basic research on steroid-induced osteonecrosis of the femoral head in Japan, J. Orthop. Sci. 21 (2016) 407–413.

[8] M.A. Mont, M.G. Zywiel, D.R. Marker, M.S. McGrath, R.E. Delanois, The natural history of untreated asymptomatic osteonecrosis of the femoral head: a systematic literature review, JBJS 92 (2010) 2165–2170.

[9] J. Moya-Angeler, A.L. Gianakos, J.C. Villa, A. Ni, J.M. Lane, Current concepts on osteonecrosis of the femoral head, World J. Orthop. 6 (2015) 590–601.

[10] S.K. Tripathy, T. Goyal, R.K. Sen, Management of femoral head osteonecrosis: current concepts, Indian J. Orthop. 49 (2015) 28–45.

[11] M.A. Mont, J.J. Cherian, R.J. Sierra, L.C. Jones, J.R. Lieberman, Nontraumatic osteonecrosis of the femoral head: where do we stand today?: a ten-year update, JBJS 97 (2015) 1604–1627.

[12] R.J.G. Renedo, M.M. Sousa, S.F. Pérez, J.R. Zabalbeascoa, L.P. Carro, Avascular necrosis of the femoral head in patients with Hodgkin's disease, Hip Int. 20 (2010) 473–481.

[13] M.A. Sahraian, S. Yadegari, R. Azarpajouh, M. Forughipour, Avascular necrosis of the femoral head in multiple sclerosis: report of five patients, Neurol. Sci. 33 (2012) 1443–1446.

[14] F.C. Zhao, K.J. Guo, Z.R. Li, Osteonecrosis of the femoral head in SARS patients: seven years later, Eur. J. Orthop. Surg. Traumatol. 23 (2013) 671–677.

[15] R.K. Aaron, A. Voisinet, J. Racine, Y. Ali, E.R. Feller, Corticosteroid-associated avascular necrosis: dose relationships and early diagnosis, Ann. N. Y. Acad. Sci. 1240 (2011) 38–46.

[16] J.L. Du, W.L. Liu, T.B. Jin, Z. Zhao, R. Bai, H. Xue, J. Chen, M. Sun, X. Zhang, G. Wang, J. Wang, A single-nucleotide polymorphism in MMP9 is associated with decreased risk of steroid-induced osteonecrosis of the femoral head, Oncotarget 7 (2016) 68434–68441.

[17] C. Hao, S.H. Yang, W.H. Xu, J.K. Shen, S. Ye, X. Liu, Z. Dong, B. Xiao, Y. Feng, MiR-708 promotes steroid-induced osteonecrosis of femoral head, suppresses osteogenic differentiation by targeting SMAD3, Sci. Rep. 6 (2016) 22599.

[18] C.X. Gu, Y. Xu, S.F. Zhang, H. Guan, S. Song, X. Wang, Y. Wang, Y. Li, G. Zhao, miR-27a attenuates adipogenesis and promotes osteogenesis in steroid-induced rat BMSCs by targeting PPAR gamma and GREM1, Sci. Rep. 6 (2016) 38491.

[19] Y. Zhang, X. Kong, R. Wang, Genetic association of the P-glycoprotein gene ABCB1 polymorphisms with the risk for steroid-induced osteonecrosis of the femoral head in Chinese population, Mol. Biol. Rep. 41 (2014) 3135–3146.

[20] Z. Wang, Y. Zhang, X. Kong, Association of a polymorphism in PON-1 gene with steroid-induced osteonecrosis of femoral head in Chinese Han population, Diagn. Pathol. 8 (2013) 186.

[21] Y. Zhang, R. Wang, S. Li, Genetic polymorphisms in plasminogen activator inhibitor-1 predict susceptibility to steroid-induced osteonecrosis of the femoral head in Chinese population, Diagn. Pathol. 8 (2013) 169.

[22] M.A. Mont, D.S. Hungerford, Current concepts review. Non-traumatic avascular necrosis of the femoral head, JBJS 77 (1995) 459–474.

[23] J. Gardeniers, ARCO committee on terminology and staging report on the committee meeting at Santiago de Compostela, ARCO Newsl. 5 (1993) 79–82.

[24] D. Szklarczyk, J.H. Morris, H. Cook, M. Kuhn, S. Wyder, M. Simonovic, A. Santos, N.T. Doncheva, A. Roth, P. Bork, L.J. Jensen, C. von Mering, The STRING database in 2017: quality-controlled protein-protein association networks, made broadly accessible, Nucleic Acids Res. 45 (2017) D362–D368.

[25] Y. Zhang, H. Wang, X. Mao, Q. Guo, W. Li, X. Wang, G. Li, N. Lin, A novel gene-expression-signature-based model for prediction of response to Tripterysium glycosides tablet for rheumatoid arthritis patients, J. Transl. Med. 16 (2018) 187.

[26] Y. Zhang, H. Wang, X. Mao, Q. Guo, W. Li, X. Wang, G. Li, Q. Jiang, N. Lin, A novel circulating miRNA-based model predicts the response to tripterysium glycosides tablets: moving toward model-based precision medicine in rheumatoid arthritis, Front. Pharmacol. 9 (2018) 378.

[27] G. Dennis, B.T. Sherman, D.A. Hosack, J. Yang, W. Gao, H.C. Lane, R.A. Lempicki, DAVID:database for annotation, visualization, and integrated discovery, Genome Biol. 4 (2003) R60.

[28] H. Ogata, S. Goto, K. Sato, KEGG: Kyoto encyclopedia of genes and genomes, Nucleic Acids Res. 27 (1999) 29–34.

[29] Y. Zhang, S. Wang, D. Li, A systems biology-based classifier for hepatocellular carcinoma diagnosis, PLoS One 6 (2011) e22426.

[30] R. Kohavi, A study of cross-validation and bootstrap for accuracy estimation and model selection, Ijcai 14 (1995) 1137–1145.

[31] L.J. Van't Veer, H. Dai, M.J. Van De Vijver, Y.D. He, A.A. Hart, M. Mao, H.L. Peterse, K. van der Kooy, M.J. Marton, A.T. Witteveen, G.J. Schreiber, R.M. Kerkhoven, C. Roberts, P.S. Linsley, R. Bernards, S.H. Friend, Gene expression profiling predicts clinical outcome of breast cancer, Nature 415 (2002) 530.

[32] L. Zhang, K. Blackwell, L.M. Workman, K.N. Gibson-Corley, A.K. Olivier, G.A. Bishop, H. Habelhah, TRAF2 exerts opposing effects on basal and TNFα-induced activation of the classic IKK complex in hematopoietic cells in mice, J. Cell Sci. 129 (2016) 1455–1467.

[33] A. Yamato, M. Soda, T. Ueno, Oncogenic activity of BIRC 2 and BIRC 3 mutants independent of nuclear factor-κB-activating potential, Cancer Sci. 106 (2015) 1137–1142.

[34] P. Wee, Z. Wang, Regulation of EGFR endocytosis by CBL during mitosis, Cells 7 (2018) E257.

[35] H.J. Cao, L.Z. Zheng, N. Wang, L.Y. Wang, Y. Li, D. Li, Y.X. Lai, X.L. Wang, L. Qin, Src blockage by siRNA inhibits VEGF-induced vascular hyperpemeability and osteoclast activity – an in vitro mechanism study for preventing destructive repair of osteonecrosis, Bone 74 (2015) 58–68.

[36] O. Basal, T. Atay, İ.M. Ciris, Y.B. Baykal, Epidermal growth factor (EGF) promotes bone healing in surgically induced osteonecrosis of the femoral head (ONFH), Bosn. J. Basic Med. Sci. 18 (2018) 352.

[37] Y. Sakamoto, T. Yamamoto, N. Sugano, D. Takahashi, T. Watanabe, T. Atsumi, J. Nakamura, Y. Hasegawa, K. Akashi, I. Narita, T. Miyamoto, T. Takeuchi, K. Ikari, K. Amano, A. Fujie, T. Kubo, Y. Tada, A. Kaneuji, H. Nakamura, T. Miyamura, T. Kabata, K. Yamaji, T. Okawa, A. Sudo, K. Ohzono, Y. Tanaka, Y. Yasunaga, S. Matsuda, Y. Imai, Japanese Research Committee on Idiopathic Osteonecrosis of the Femoral Head, M. Akiyama, M. Kubo, Y. Kamatani, Y. Iwamoto, S. Ikegawa, Genome-wide association study of idiopathic osteonecrosis of the femoral head, Sci. Rep. 7 (2017) 15035.

[38] S.B. Ferreira Jr., C.E. Repeke, F.M. Raimundo, I.S. Nunes, M.J. Avila-Campos, B.R. Ferreira, J. Santana da Silva, A.P. Campanelli, G.P. Garlet, CCR5 mediates pro-osteoclastic and osteoclastogenic leukocyte chemoattraction, J. Dent. Res. 90 (2011) 632–637.

[39] J.W. Lee, A. Hoshino, K. Inoue, T. Saitou, S. Uehara, Y. Kobayashi, S. Ueha, K. Matsushima, A. Yamaguchi, Y. Imai, T. Iimura, The HIV co-receptor CCR5 regulates osteoclast function, Nat. Commun. 8 (2017) 2226.

[40] X. Liu, Q. Li, X. Niu, B. Hu, S. Chen, W. Song, J. Ding, C. Zhang, Y. Wang, Exosomes secreted from human-induced pluripotent stem cell-derived mesenchymal stem cells prevent osteonecrosis of the femoral head by promoting angiogenesis, Int. J. Biol. Sci. 13 (2017) 232.

[41] S. Okazaki, Y. Nishitani, S. Nagoya, M. Kaya, T. Yamashita, H. Matsumoto, Femoral head osteonecrosis can be caused by disruption of the systemic immune response via the toll-like receptor 4 signalling pathway, Rheumatology 48 (2009) 227–232.

[42] U.M. zum Büschenfelde, L.I. Brandenstein, L. von Elsner, K. Flato, T. Holling, M. Zenker, G. Rosenberger, K. Kutsche, RIT1 controls actin dynamics via complex formation with RAC1/CDC42 and PAK1, PLoS Genet. 14 (2018) e1007370.

[43] B. Song, Y. Chi, X. Li, W.J. Du, Z.B. Han, J.J. Tian, J.J. Li, F. Chen, H.H. Wu, L.X. Han, S.H. Lu, Y.Z. Zheng, Z.C. Han, Inhibition of Notch signaling promotes the adipogenic differentiation of mesenchymal stem cells through autophagy activation and PTEN-PI3K/AKT/mTOR pathway, Cell. Physiol. Biochem. 36 (2015) 1991–2002.

[44] S. Mollazadeh, B.S. Fazly Bazzaz, M.A. Kerachian, Role of apoptosis in pathogenesis and treatment of bone-related diseases, J. Orthop. Surg. Res. 10 (2015) 15.

[45] Y. Han, M. Si, Y. Zhao, Y. Liu, K. Cheng, Y. Zhang, J. Jia, J. Li, L. Nie, Progranulin protects against osteonecrosis of the femoral head by activating erk1/2 pathway, Inflammation 40 (2017) 946–955.

[46] N.S. Adapala, R. Yamaguchi, M. Phipps, O. Aruwajoye, H.K.W. Kim, Necrotic bone stimulates proinflammatory responses in macrophages through the activation of toll-like receptor 4, Am. J. Pathol. 186 (2016) 2987–2999.

[47] M. Wang, G. Yan, Z. Fei, Kernel PLS based prediction model construction and simulation on theoretical cases, Neurocomputing 165 (2015) 389–394.